Theoretical and Experimental Studies of Molecular Geometry, Orbitals, and Vibrational Spectra of Bioactive 3,7-Dinitrodibenzobromolium Cation

Xin Huai Zhang* and Yuan Ping Feng

Department of Physics, National University of Singapore, Singapore 119260

Zi Jie Hou

Department of Chemistry, Lanzhou University, Lanzhou 730000, China

Received: March 30, 1998

A comprehensive investigation of molecular structure and electronic properties of bioactive 3,7-dinitrodibenzobromolium cation was carried out using ab initio calculation and IR and Raman spectroscopic studies. Geometric optimization of the 3,7-dinitrodibenzobromolium cation was performed using the restricted Hartree−Fock method with different basis sets. The resulting molecular structure agrees very well with X-ray diffraction data. Middle-infrared IR spectra and Raman spectra of the 3,7-dinitrodibenzobromolium bisulfate were obtained, and its fundamental vibrations were assigned and compared with the theoretical predictions. The agreement between the calculated and experimental frequencies is excellent, except for the symmetric and asymmetric vibration frequencies of the nitro group which show relatively larger discrepancies between the calculated and experimental results. This can be attributed to the neglect of the electron correlation in the HF method and neglect of the crystal packing force and counterion effects in the theoretical calculation.

1. Introduction

In recent years, much attention has been given to the quantitative structure−activity relationship (QSAR) method in finding new drugs, and many successful applications have been reported. QSAR has played major roles in the designs of some compounds which have been commercialized and others which have reached later stages of development.[1] Since the activity of a drug molecule is closely related to its electronic structure, investigation of the electronic structure of a drug molecule can provide a close insight into the mechanism of the action of the drug. The ability to accurately and routinely calculate a wide range of molecular properties is one of the most important practical advances that have occurred in molecular electronic structure theory over the past quarter century.[2] A whole spectrum of theoretical methods, from the simple molecular mechanics to the advanced ab initio, quantum mechanics calculation, has been developed and has been available not only to researchers but also to modern drug design laboratories. These properties that can be obtained by theoretical methods include molecular energy, dipole moment, polarizability, electron potential, atomic charge distribution, molecular geometry, and vibrational frequencies.[3]

Since they were first synthesized in the 1950s,[4] iodine heterocyclic compounds have attracted considerable research and clinical interest. It has been shown that compounds containing iodine atoms have a wide range of biological activities, such as antihypertensive, antiradiation, bacteriostasis, and antiarrhythinic effects,[5] and some of them were found to be highly effective in treating tumor cells in vitro.[6] Recently similar compounds containing bromine atoms have been successfully synthesized. Preliminary study has shown that these compounds are also biologically active and possess an immunity enhancement effect.[7] However, despite the vast experimental studies on the structure and biological activities of these iodine and bromine heterocyclic compounds, there has been no theoretical investigation on the fundamental properties of these molecules to date. The mechanisms of interaction between the molecules and the target DNA or protein remain unknown. It is therefore the aim of our present research efforts to investigate systematically the series of bromine and iodine heterocyclic compounds, to calculate and measure their properties and structures, to test their biological activities, and to draw a quantitative structure−activity relationship for the series of compounds. In addition, to provide theoretical understanding of the properties and the origins of biological activities based on fundamental physical laws, it is hoped that such studies will provide a guideline for further improvements on the activities of these compounds and in the designs of new drugs based on similar compounds. The 3,7-dinitrodibenzobromolium cation (Figure 1) is the first in the series of molecules which are being studied. In this article, we report the basic properties of this molecule determined from ab initio calculation and IR and Raman spectroscopic studies.

2. Method

2.1. Ab Initio Calculation. In this study, we employed the restricted Hartree−Fock (RHF) method as it is implemented in the Gaussian 94 program.[8] Within the constraint of available computer resources, only the cation was considered in the ab initio calculation. Even though the compound exists in crystalline form, the above treatment is validated by the fact that an ionic bond is formed between the 3,7-dinitrodibenzobromolium cation and the bisulfate anion, as indicated by the X-ray diffraction data.[7]

Different basis sets, including the STO-3G, 3-21G, 3-21G**, 6-31G*, and 6-31G**, were used in the calculation, and the

* To whom correspondance should be addressed. E-Mail: scip6095@leonis.nus.edu.sg.

10.1021/jp981674n CCC: $15.00
Published on Web 10/27/1998

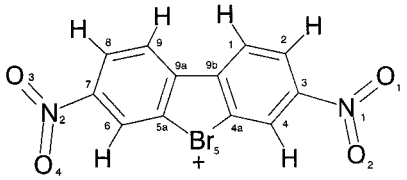

Figure 1. Structure of the 3,7-dinitrodibenzobromolium cation.

results were compared with X-ray diffraction data in order to determine the most appropriate combination for the given molecular system and other similar molecules to be studied. The calculation was performed on the Cray J916 supercomputer at the National University of Singapore.

In addition to the constraint-free, full structural optimization, we have also performed structural minimizations by imposing various symmetry constraints, such as C_s, C_2, and C_{2v}, respectively, in order to explore the effects of symmetry constraint on the geometry optimization. The convergence criteria used here are as follow: (1) The cutoff value for the maximum component of the force is 0.00045. (2) The root mean square of the force is below 0.0003. (3) The cutoff value for the calculated displacement of the next step is 0.0018. (4) The root mean square for the displacement of the next step is below 0.0012.

The optimization for all of the structures converged. The frequencies analysis for the optimized structures found no imaginary frequecies, which means that they are all structural minima. These optimized structures are basically the same, with differences in total energies being less than 9.4×10^{-3} kcal/mol. The differences in bond lengths and bond angles between the structures optimized with different symmetries are less than 0.0003 Å and 0.02°, respectively. Furthermore, the differences become even smaller as more stringent convergence criteria were used in the calculation. We can, therefore, conclude that the symmetry constraint imposed during structural optimization has little effect on the equilibrium structure of the cation. Nevertheless, when using the 6-31G** basis set and imposing the C_{2v} symmetry, we obtained the lowest single point energy and the best agreement between the calculated and the experimental structural parameters. On the basis of this, we present the molecular structure optimized with the C_{2v} symmetry constraint and various basis sets. The molecular orbitals and the vibrational frequencies of the 3,7-dinitrodibenzobromolium cation were calculated using the 6-31G** basis set on the geometry of RHF/6-31G**.

2.2. IR and Raman Measurements. The 3,7-dinitrodibenzobromolium bisulfate used in the experiments was prepared as described in ref 7. X-ray diffraction data (XRD) for the crystalline form of the 3,7-dinitrodibenzobromolium bisulfate has been obtained previously. Various geometric parameters calculated in the present study were directly compared with the available XRD data.[7] The IR spectrum was recorded from 400 to 5000 cm^{-1} with a resolution of 4 cm^{-1} using the KBr-pellet technique with a PE 2000 FT-IR spectrometer. The spectrum was taken ex situ in transition mode. The Raman spectrum was collected in the backscattering geometry using a Renishaw System 2000 Ramascope. The 782 nm line of a laser diode (LD) was used as the excitation source, and the power at the sample was estimated to be below 20 mW. Raman scattering light was collected by a charge coupled device (CCD) detector. The measurement was performed at room temperature and ambient atmosphere. The spectral resolution is about 2 cm^{-1}.

TABLE 1. Comparison of Bond Lengths (Å) Obtained from ab Initio Calculation with Various Basis Sets and Those Determined by XRD

bond	6-31G*	6-31G**	expt
$r_{C_{5a}-C_{9a}}$	1.388	1.388	1.376
$r_{C_{9b}-C_{9a}}$	1.469	1.469	1.456
$r_{C_{4a}-C_{9b}}$	1.388	1.388	1.377
$r_{C_9-C_{9a}}$	1.388	1.388	1.395
$r_{C_6-C_{5a}}$	1.368	1.368	1.369
$r_{C_8-C_9}$	1.386	1.386	1.377
$r_{C_7-C_6}$	1.384	1.384	1.372
$r_{C_7-C_8}$	1.383	1.383	1.390
$r_{C_1-C_{9b}}$	1.388	1.388	1.389
$r_{C_1-C_2}$	1.386	1.385	1.392
$r_{C_4-C_{4a}}$	1.368	1.368	1.360
$r_{C_2-C_3}$	1.383	1.383	1.369
$r_{C_3-C_4}$	1.384	1.384	1.399
$r_{C_5-C_{5a}}$	1.930	1.930	1.912
$r_{C_5-C_{4a}}$	1.930	1.930	1.926
$r_{N_2-C_7}$	1.463	1.464	1.454
$r_{N_1-C_3}$	1.463	1.464	1.469
$r_{O_3-N_2}$	1.187	1.187	1.206
$r_{O_4-N_2}$	1.191	1.191	1.224
$r_{O_2-N_1}$	1.187	1.187	1.203
$r_{O_1-N_1}$	1.191	1.191	1.201

TABLE 2. Comparison of Bond Angles (deg) Obtained from ab Initio Calculation with Various Basis Sets and Those Determined by XRD

angle	6-31G*	6-31G**	expt
$A_{C_{5a}C_{9a}C_{9b}}$	115.6	115.6	115..3
$A_{C_{4a}C_{9b}C_{9b}}$	115.6	115.6	115.4
$A_{C_9C_{9a}C_{5a}}$	116.6	116.6	116.7
$A_{C_6C_{5a}C_{9a}}$	126.2	126.2	126.3
$A_{C_8C_9C_{9a}}$	120.0	120.0	120.3
$A_{C_7C_8C_9}$	119.9	119.8	118.9
$A_{C_6C_7C_8}$	122.7	122.8	123.6
$A_{C_1C_{9b}C_{4a}}$	116.6	116.6	117.3
$A_{C_4C_{4a}C_{9b}}$	126.2	126.2	126.7
$A_{C_5C_{5a}C_{9a}}$	110.7	110.7	110.8
$A_{C_5C_{4a}C_{9b}}$	110.7	110.7	111.1
$A_{C_{4a}C_5C_{5a}}$	87.4	87.4	86.7
$A_{C_7N_2O_3}$	116.9	116.9	119.9
$A_{C_7N_2O_4}$	116.6	116.6	118.2
$A_{O_3N_2O_4}$	126.5	126.5	122.7
$A_{C_3N_1O_2}$	126.9	116.9	118.8
$A_{C_3N_1O_1}$	116.6	116.6	118.5
$A_{O_1N_1O_2}$	126.5	126.5	122.7

TABLE 3. Root Mean Square of the Differences between the Experimental Parameters and the Theoretical Values for Each Basis Set Considered

	STO-3G	3-21G	3-21G**	6-31G*	6-31G**
bond length	0.037	0.021	0.017	0.014	0.013
bond angle	2.29	1.76	1.69	1.55	1.51

3. Results and Discussion

3.1. Molecular Structure. The bond lengths and the bond angles of structures optimized with 6-31G* and 6-31G** basis sets are listed in Table 1 and Table 2, respectively. The experimental data obtained from X-ray diffraction[7] are also listed for comparison. It can be seen in Table 1 and Table 2 that the level of the agreement between the theoretical and experimental results is excellent.

Results obtained using different basis sets are also close. For a quantitative comparison, we calculated the root mean square (rms) of the differences between the experimental parameters and the theoretical values for each basis set considered (Table 3). As expected, the accuracy of calculation increases monotonically when larger basis sets are used. However the improvements are only marginal. Using the minimal basis set,

TABLE 4. Bond Lengths (Å) That Are Most Affected by the Nitro Group Rotation around the C−N Bond and Associated Energy Barriers for Various Dihedral Angles of Rotation

dihedral angle (deg)	energy barrier (kcal/mol)	Bond Length (Å)					
		$r_{C_3-N_1}$	$r_{N_1-O_1}$	$r_{N_1-O_2}$	$r_{C_7-N_2}$	$r_{N_2-O_3}$	$r_{N_2-O_4}$
0		1.4636	1.1868	1.1905	1.4636	1.1905	1.1868
2	0.0314	1.4635	1.1868	1.1905	1.4635	1.1905	1.1868
5	0.0628	1.4634	1.1868	1.1905	1.4633	1.1905	1.1868
10	0.2510	1.4630	1.1869	1.1905	1.4630	1.1905	1.1869
30	2.5104	1.4602	1.1874	1.1905	1.4602	1.1905	1.1873
90	15.8783	1.4619	1.1876	1.1876	1.4620	1.1876	1.1876

STO-3G, the largest difference between the theoretical and experimental bond lengths is only 0.077 Å, which occurs in the O_1-N_1 bond, while the largest difference in bond angles is 3.3° (the $O_1-N_1-O_2$ and $O_3-N_2-O_4$ bonds). The results obtained with the polarized basis sets 6-31G* and 6-31G** are almost identical and represent the best agreement with experimental values among all the basis sets considered. The largest deviation occurred in the O_4-N_2 bond, where the calculated bond length is 1.191 Å and that of the XRD measurements is 1.224 Å. The largest deviation in bond angle was found in the O−N−O angles in the nitro groups. This angle in both nitro groups is 3.8° larger than the experimental value of 122.7°.

Larger discrepancies are generally found in bond lengths and bond angles involving atoms in the nitro groups. Using the minimal basis set, the resulting bond lengths are consistently larger than the corresponding experimental values. On the other hand, short bonds were obtained using the polarized basis sets, with the only exception being the N_2-C_7 bond. The split-valence basis sets, 3-21G and 3-21G* produced longer O−N bonds and shorter C−N bonds. The deviations in bond angles are more consistent. For all the basis sets used in the calculation, the C−N−O bond angles are generally smaller, while the O−N−O bond angles are larger than the corresponding experimental values.

Furthermore, it was observed in the structure depicted by XRD data that the two nitro groups are not in the same plane with the benzene rings, but rather they are rotated slightly around the C−N bonds. However, the nitro groups are found in the same plane with the benzene rings in the structure obtained by computational optimization. In the planar molecule, it is believed that a conjugation is formed between a nitro group and the benzene ring to which it is attached, and rotation of the nitro group around the C−N bond may disrupt this conjugation. Polittzer et al. have investigated the structural effect of the nitro group rotation around the C−N bond and found that the rotation resulted in a shortening of the N−O bond and elongation of the C−N bonds, confirming the conjugation between the nitro group and the benzene ring.[9] In the present work, we carried out further structural optimization of the molecule with a fixed dihedral angle between the nitro group and the benzene ring, in order to investigate the effect of the rotation of the nitro group on the geometry parameters. The most affected bond lengths by this rotation are given in Table 4. It is found that, for the angle of rotation of less than 30°, the C−N bonds are shortened slightly, while almost no noticeable changes to the N−O bonds were found. Little changes were also found in the bond angles and are not listed here. The larger discrepancies between the calculated and the experimental O−N−O bond angles persist in the structure obtained by the constrained optimization. This indicates that the effect of the conjugation between the nitro group and the benzene ring, if it exists, to the molecular structure of the 3,7-dinitrodibenzobromolium cation is negligible and the discrepancies between the calculated and optimized geometric parameters are due mostly to the neglect of the electron correlation in the HF method. For organic nitro compounds this neglect can cause large deviations in the molecular geometric parameters.[10]

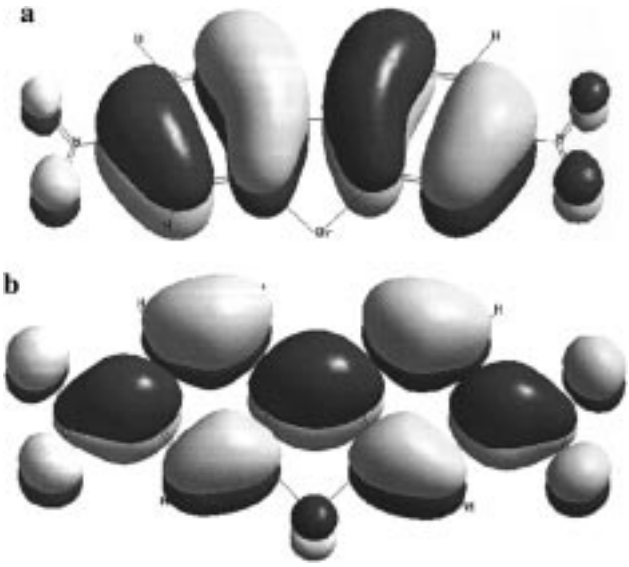

Figure 2. (a) Highest occupied molecular orbital (energy: −0.507 88 hartrees) and (b) lowest unoccupied molecular orbital (energy: −0.131 86 hartrees) of the optimized 3,7-dinitrodibenzobromolium cation.

Figure 3. Orbital number 62 of the optimized 3,7-dinitrodibenzobromolium cation (energy: −0.781 64 hartrees). A large π bond is formed among the benzene rings and the bromine atom.

3.2. Molecular Orbitals. The molecular orbitals were obtained using the 6-31G** basis set for the optimized molecular structure. A total of 312 molecular orbitals were formed, 79 of which are occupied. The highest occupied molecular orbital (HOMO) and the lowest unoccupied molecular orbital (LUMO) are shown in Figure 2a,b, respectively. The HOMO is characterized by large π bonds among different C atoms. The Br and the N atoms do not contribute to the formation of these bonds. The LUMO is also characterized by some π bonds among the carbon atoms. A π bond between the carbon atom and the nitrogen atom is noticeable.

Another interesting molecular orbital is orbital no. 62, which is shown in Figure 3. This is an occupied bonding orbital. Here all the carbon atoms and the bromine atom are involved, and each of them provides a p orbital which is in phase with one another. Therefore a large π bond is formed among all the carbon atoms and the bromine atom. Although this orbital may not contribute to the bonding of the molecule because it is not a valence bond orbital, its shape indicates that electronic correlation exists among these atoms. Another π bond is formed in each of the nitro groups in the same orbital.

The molecular orbitals corresponding to the HOMO and the LUMO shown in Figure 2, for the structure obtained from optimization with a constrained dihedral angle between the nitro group and the benzene ring, are shown in Figure 4a,b, for a

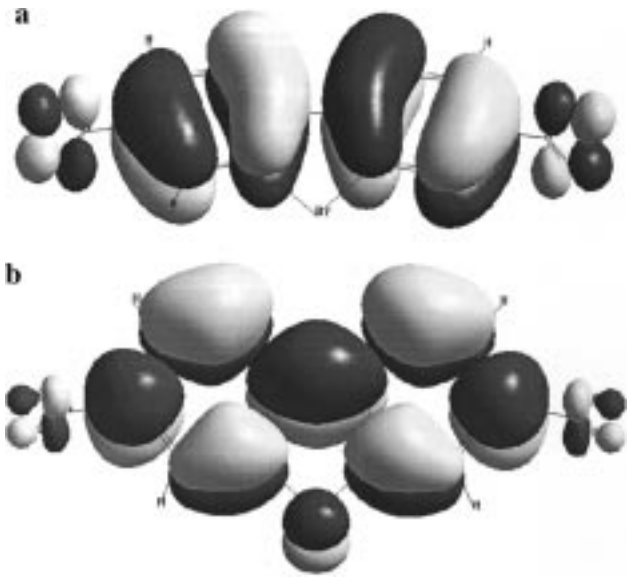

Figure 4. Molecular orbital corresponding to those shown in Figure 2, of the structure obtained by fixing the dihedral angle between the nitro group and the benzene ring to 90° during optimization. (a) HOMO (energy: −0.499 82 hartrees); (b) LUMO (energy: −0.107 27 hartrees).

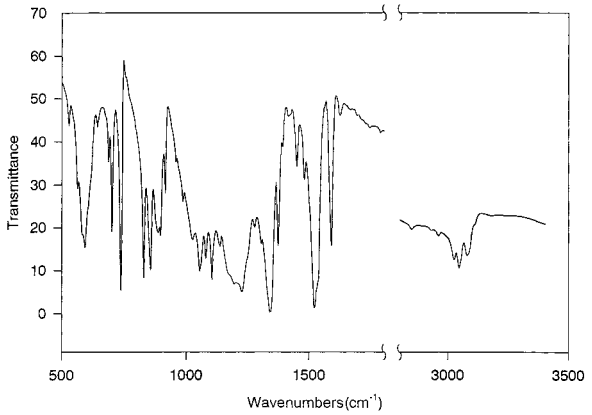

Figure 5. IR spectrum of the 3,7-dinitrodibenzobromolium bisulfate.

dihedral angle of 90°. It can be seen that the central part of the HOMO is not affected by the rotation of the nitro group and remains the same as in Figure 2a. However the nitro π bond is broken which causes a rise in the energy of the orbital. The same phenomenon is observed in the LUMO of the molecule. Here the π bond between the carbon atom and the nitrogen atom is broken due to the nitro group rotation. This causes the energy of this orbital to be higher than that of the orbital immediately above previously and becomes orbital number 81 (LUMO+1). On the other hand, the orbital previously above the LUMO was not affected by the nitro group rotation and takes over the role of LUMO.

A π bond is formed between the N atom and the nearest C atom (Figure 2b). This bond is twisted when the nitro group is rotated and eventually is broken when the angle of the rotation becomes large enough. However due to the fact that this is an unoccupied molecular orbital, the resulting energy barrier is small (Table 4).

3.3. IR and Raman Spectroscopy. The experimental IR and Raman spectra of the 3,7-dinitrodibenzobromolium bisulfate are shown in Figure 5 and Figure 6, respectively. The measured fundamental frequencies and mode assignments are listed in Table 5, together with those harmonic vibrational frequencies obtained from theoretical vibrational analysis which was carried

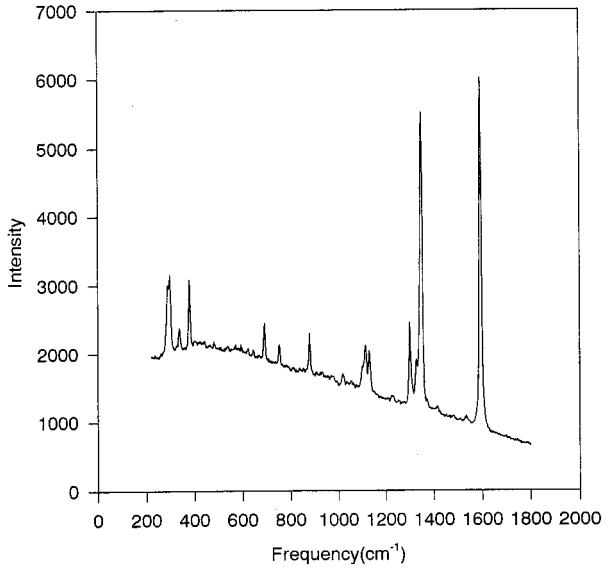

Figure 6. Raman spectrum of the 3,7-dinitrodibenzobromolium bisulfate.

out using the 6-31G** basis set for geometry obtained with the RHF/6-31G** method.

The 3,7-dinitrodibenzobromolium cation with the C_{2v} symmetry has 59 normal vibrational modes of various symmetries ($24A_1 + 11A_2 + 11B_1 + 23B_2$). Among these the A_2 symmetry vibrations are IR inactive, while all the vibrations are Raman active. However, due to the limited range of the observed bands, only those frequencies above 600 cm^{-1} are assigned unambiguously. A few IR bands were not observed in our measurement due to the low intensity and limited resolution of the spectra. And the fact that fewer lines are observed in Raman spectra precludes a one-to-one correspondence between the theoretical and the observed Raman bands.

The frequencies predicted by the RHF/6-31G** method have been scaled by an empirical factor of 0.8992, which was recommended by Scott and Radom[11] in order to remove the systematic error of RHF/6-31G** method. The major source of this error comes from the neglect of anharmonicity effects in the theoretical treatment. The neglect of electron correlation effects and the use of the finite basis sets in the HF method also contribute to the disagreement between the observed fundamentals and the predicted harmonic frequencies. Although the higher the frequencies, the larger the anharmonicity, the overall overestimation of the HF method is relatively uniform.[11] So we used a generic frequency scaling factor to scale our predicted harmonic frequencies.

The mode assignments are made according to the amplitudes of atomic motions at the given frequency and with reference to ref 12. The calculated frequencies for various vibrational modes are generally in good agreement with those obtained in the IR and Raman experiments. The rms values of the differences between the calculated and experimental frequencies are 19 and 16 cm^{-1} for IR and Raman, respectively. The calculated frequencies for the symmetric and asymmetric vibrations of the nitro group are still 39 and 178 cm^{-1} larger than the observed frequencies for IR and 124 and 29 cm^{-1} larger for Raman, even after scaling by 0.8992, and they are not included in the calculation of the rms values. Poor predictions of vibrational frequencies for certain multiple-bond systems (e.g., N_2, O_2, and O_3) and organic nitro compounds which have strong electron correlations seem typical of the HF and MP2 levels of theory.[10,11,13,14] Using density functional theory method, Jursic[10]

TABLE 5. Comparisons between the Calculated and the Experimental IR and Raman Frequencies (cm^{-1})

		IR freq				Raman freq					
no.[a]	sym	theor	IR intens[b]	expt	rel intens[c]	theor	Raman intens[d]	expt	rel intens[d]	depol[e]	mode description[f]
24	B_2	628	23.1	592	s	628	3.9	–[g]		0.75	CH ip bend
25	A_1	666	16.4	641	w	666	9.3	–		0.10	CH bend,ring defm
26	B_1	683	1.5	686	m	683	3.6	690	m	0.75	CH opp bend
27	B_2	685	96.1	700	s	685	0.3	–		0.75	NO_2 defm
28	A_2	725	0.0			725	1.2	–		0.75	CH oop bend
29	B_1	759	92.7	736	s	759	0.3	–		0.75	CH,CN oop bend
30	A_1	760	1.4	–		760	4.5	–		0.12	NO_2 defm
31	A_2	767	0.0			767	14.6	753	m	0.12	NO,CH oop bend
32	B_2	860	79.5	828	s	860	0.0	–		0.75	NO_2 defm,CH bend
33	A_1	867	39.0	856	s	867	1.5	–		0.75	CH oop bend
34	A_1	881	10.6	886	m	881	24.4	878	m	0.11	NO_2 defm
35	A_2	883	0.0			883	0.2	–		0.75	CH oop bend
36	A_2	951	0.0			951	5.9	–		0.75	CH oop bend
37	B_1	953	31.6	915	m	953	0.5	–		0.75	CH oop bend
38	B_2	966	30.6	985	m	966	0.5	–		0.75	ring defm,CH bend
39	A_1	999	16.6	1022	m	999	9.8	–		0.09	ring defm,CH bend
40	A_2	1020	0.0			1020	4.3	1017	w	0.75	CH oop bend
41	B_1	1122	0.4	–		1122	0.0	–		0.75	CH oop bend
42	B_2	1043	0.0	–		1043	0.0	–		0.75	CH ip bend
43	B_2	1091	2.5	1078	s	1091	3.5	–		0.75	CC str
44	A_1	1106	0.2	–		1106	3.6	1101	w	0.47	CH ip bend
45	B_2	1120	110.0	1107	s	1120	0.2	–		0.75	CH ip bend
46	A_1	1124	1.3	–		1124	61.3	1115	m	0.21	CH ip bend
47	A_1	1153	21.7	1130	m	1153	49.8	1130	m	0.30	CC, CH bend
48	B_2	1180	25.6	1170	s	1180	8.4	–		0.75	CH ip bend
49	A_1	1245	14.8	1229	s	1245	3.4	–		0.23	CH ip bend
50	B_2	1255	9.1	1281	m	1255	0.2	–		0.75	CH ip bend
51	A_1	1294	0.0	–		1294	233.8	1300	s	0.24	CH ip bend
52	A_1	1367	41.1	1375	m	1367	11.8	1326	m	0.13	CH ip bend
53	B_2	1407	1.8	1398	w	1407	4.7	–		0.75	CH ip bend
54	B_2	1455	469.7	1449	w	1455	0.1	–		0.75	CH bend,CN str
55	A_1	1473	7.6	1341	m	1473	237.4	1349	vs	0.18	NO_2 sym str
56	B_2	1481	336.1	1342	vs	1481	0.0	–		0.75	NO_2 sym str
57	A_1	1499	3.8	–		1499	2.7	–		0.63	ring tor
58	A_1	1572	54.0	1537	s	1572	42.4	–		0.27	ring str
59	B_2	1582	5.3	–		1582	1.62	–		0.75	ring tor
60	B_2	1614	7.1	1591	m	1614	0.13	–		0.75	ring str
61	A_1	1622	1.0	1591	m	1622	1210.5	1593	vs	0.37	ring str
62	B_2	1703	20.6	1525	vs	1703	5.7	–		0.75	NO_2 asym str
63	A_1	1703	859.5	1525	vs	1703	0.3	–		0.10	NO_2 asym str
64	B_2	3048	0.0	3026	s	3048	12.7	–		0.75	CH str
65	A_1	3055	0.0	3027	s	3055	58.7	–		0.36	CH str
66	B_2	3073	20.2	3045	s	3073	26.0	–		0.75	CH str
67	A_1	3073	40.1	3046	s	3073	71.4	–		0.11	CH str
68	B_2	3075	15.6	3078	s	3075	53.0	–		0.75	CH str
69	A_1	3076	16.8	3079	s	3076	144.9	–		0.11	CH str

[a] Number in the order from the calculated results. [b] IR intensity: km/mol. [c] Relative intensity: vs, very strong; s, strong; m, medium; w, weak. [d] Raman intensity: A^4/amu. [e] Depolorization ratio. [f] str = stretch; bend = bending; wag = wagging; tor = torsion; defm = deformation; ip = in-plane; oop = out-of-plane. [g] Frequency not observed due to the low intensity and limited resolution.

has obtained better agreement between the calculated and the experimental vibration frequencies for the singlet nitromethane. Therefore, a similar treatment could improve the calculated vibrational frequencies in the nitro groups. This will be considered in further investigation. In our case, another source of error might be due to the fact that the crystal of the compound was used in the experiments, while the theoretical analysis was performed only on the cation in the gaseous form where the crystal packing force and counterion effects are neglected.

3.4. Mulliken Charges. The charge distribution of a molecular system is of great importance to its structure and activity.[15] Mulliken population analysis was carried out for the planar 3,7-dinitrodibenzobromolium cation as well as that optimized with the constrained dihedral angle between the nitro group and the benzene ring. The calculated charge distributions are shown in Figure 7a for the planar molecule and Figure 7b for the structure optimized with the dihedral angle being constrained to 90°.

In both cases, the positive charge centers are at the bromine atom and the nitrogen atoms, while the negative charge centers are at the oxygen atoms. The rotation of the nitro group affected the charge distributions in the nitro groups, and those of the carbon atoms to which the nitro groups are attached, as well as the nearby hydrogen atoms. This is partially due to the rearrangements of the electronic density arising from the different nuclear configuration and partially due to the reduced interactions between the hydrogen atoms and the oxygen atoms

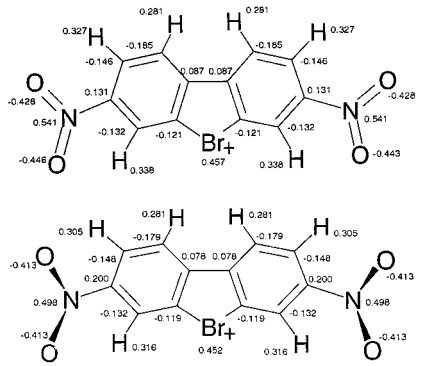

Figure 7. Mulliken charge distribution of the 3,7-dinitrodibenzobromolium cation: (a) the planar molecular structure; (b) the structure optimized with the dihedral angle between the nitro group and the benzene ring being fixed to 90°.

as the oxygen atoms have moved away from the hydrogen atoms by the rotation.

4. Conclusion

The molecular structure of the 3,7-dinitrodibenzobromolium cation is investigated using the restricted Hartree−Fock method with different basis sets. The fully optimized molecular structure is compared with that determined by X-ray diffraction. Better agreement between the predicted bond length and bond angles and the corresponding experimental values is obtained as an increasingly larger basis set is used. However, the improvement is marginal. Relatively larger discrepancies are found between the theoretical and the experimental parameters in the nitro groups. This is mainly due to the neglect of the electron correlation in the HF method. Crystal packing force and counterion effects which were neglected in the present ab initio calculation may also contribute to a certain degree to the discrepancies between the calculated and experimental bond lengths and bond angles in the nitro group. The electronic structure calculation also shows that the nitro groups do not form conjugations with the central benzene rings.

We also carried out vibrational analysis of the cation. The predicted frequencies for various vibrational modes compare fairly well to those determined by IR and Raman spectroscopies. However, the vibrational frequencies pertaining to the nitro group have larger deviations compared to the experimental value. This can also be attributed to the neglect of the electron correlation in the HF method and the neglect of the crystal packing force and the counterion effect in the theoretical treatment.

Acknowledgment. The authors wish to thank the Supercomputer and Visualization Unit, National University of Singapore, for providing the computer resources and Dr. Grace Foo for technical assistance. The authors also wish to thank Dr. Z. Shen, Xianbin Wang, and Luwei Chen for their assistance in the IR and Raman spectroscopic measurements and useful discussions.

References and Notes

(1) Herrmann, E. C., Frank, R. Eds. *Computer Aided Drug Design in Industrial Research*; Springer-Verlag: Berlin, 1995.

(2) Mart, H. *J. Phys. Chem.* **1996**, *100*, 13213.

(3) Warren, J. H.; Leo, R.; Paul, S.; John, A. P. *Ab initio Molecular Orbital Theory*; John Wiley & Sons Inc.: New York, 1986.

(4) Huang, W. *Huaxue Xuebao* **1956**, *22*, 292 (in Chinese).

(5) Chen, S.; Wang, C.; Li, D.; Wang, X. *Sci. China, Ser. B* **1986**, *32*, 918.

(6) Liu, L.; Zheng, R.; Hou, Z. *Kexue Tongbao* **1989**, *10*, 783 (in Chinese).

(7) Hou, Z.; Zhu, Y.; Wang, Q. *Sci. China, Ser. B* **1996**, *39*, 262.

(8) Frisch, M. J.; Trucks, G. W.; Schlegel, H. B.; Gill, P. M. W.; Johnson, B. G.; Robb, M. A.; Cheeseman, J. R.; Keith, T.; Petersson, G. A.; Montgomery, J. A.; Raghavachari, K.; Al-Laham, M. A.; Zakrzewski, V. G.; Ortiz, J. V.; Foresman, J. B.; Cioslowski, J.; Stefanov, B. B.; Nanayakkara, A.; Challacombe, M.; Peng, C. Y.; Ayala, P. Y.; Chen, W.; Wong, M. W.; Andres, J. L.; Replogle, E. S.; Gomperts, R.; Martin, R. L.; Fox, D. J.; Binkley, J. S.; Defrees, D. J.; Baker, J.; Stewart, J. P.; Head-Gordon, M.; Gonzalez, C.; Pople, J. A. *Gaussian 94*, Revision C; Gaussian, Inc.: Pittsburgh, PA, 1995.

(9) Politzer, P.; Lane, P.; Jayasuriya, K.; Domelsmith, L. N. *J. Am. Chem. Soc.* **1987**, *109*, 1899.

(10) Jursic, B. S. *Int. J. Quantum Chem.* **1997**, *64*, 263.

(11) Scott, A. P.; Radom, L. *J. Phys. Chem.* **1996**, *100*, 16502.

(12) Colthup, N. B.; Daly, L. H.; Wiberley, S. E. *Introduction to Infrared and Raman Spectroscopy*, 2nd ed.; Academic Press, Inc.: New York, 1975.

(13) Pople, J. A.; Scott, A. P.; Wong, M. W.; Radom, L. *Isr. J. Chem.* **1993**, *33*, 345.

(14) Wong, M. W. *Chem. Phys. Lett.* **1996**, *256*, 391−399.

(15) Grimes, R. N. *Carboranes*; Academic Press: New York, 1970.